A Slip Detection and Correction Strategy for Precision Robot Grasping

Michael Stachowsky, Thomas Hummel, Medhat Moussa, and Hussein A. Abdullah

***Abstract*—This paper presents a grasp force regulation strategy for precision grasps. The strategy makes no assumptions about object properties and surface characteristics, and can be used with a wide range of grippers. It has two components, a slip signal detector that computes the magnitude of slip and a grasping force set point generator that acts on the detector's output. The force set point generator is designed to ensure that slip is eliminated without using excessive force. This is particularly important in several situations like grasping fragile objects or in-hand manipulation of thin small objects. Several experiments were conducted to simulate various grasping scenarios with different objects. Results show that the strategy was very successful in dealing with uncertainty in object mass, surface characteristics, or rigidity. The strategy is also insensitive to robot motion.**

***Index Terms*—Grasping, robot control, tactile sensors.**

I. Introduction

PERFORMING a successful grasp of a known rigid object is a well-studied problem (see [1], for a comprehensive treatment of the subject). If the object is unknown or there is uncertainty in the object characteristics (e.g., center of mass, surface friction), then the problem is more difficult. Recent advances in compliant, underactuated hands have simplified the problem of executing a power grasp even with considerable uncertainty [2]–[4]. Yet there are many tasks beyond simple pick and place where precision grasps are necessary and where dexterity and manipulation play a central role. In some manipulation tasks, precision grasps are necessary. For example, consider grasping a key that is left on a table to be inserted into a lock. The hand must grasp the key with a pinch grasp, since it is thin, and then, rotate the key in the hand to have better contact surface in order to push it into the lock. Bennet notes that "...the purpose of a precision grasp is generally to provide dexterity" [5]. Typically, low-precision systems are used for gross motions and power grasping. Some general work has been done to increase the precision of low precision systems [6]. However, even with a high precision, fully articulated hand, dexterous manipulation remains a challenging task.

Power grasps are generally very stable while precision grasps emphasize dexterity and sensitivity over stability [7]. Thus, while power grasps do not typically require complex grasp force regulation, force regulation is important for precision grasps especially where grasping is followed by manipulation. This is also complicated by the fact that initial grasping forces could reorient the object, especially if it is thin. Thus, it is important to have on-line regulation of grasping forces.

Another scenario where precision grasps with online force regulation is needed is when the object is nonrigid and fragile. For example, grasping a strawberry or a mushroom during a harvest operation requires delicate balance of grasping forces. Applying too high a force could damage the quality of the fruit and reduce its shelf life while too low a force would mean that slippage would occur and the grasp would fail. This problem has recently generated significant industry interest (see [8]–[10]).

Finally, a similar case can be made when grasping a crushable object with dynamic mass such as a Styrofoam cup. In this case, the cup may or may not have liquid in it. When the cup is empty, grasping forces must only balance the weight of the cup. If the cup is full, then using the same grasping forces as if it were empty will obviously fail to hold the cup due to the weight of the liquid. Yet it is not feasible to preprogram the grasping forces assuming that the cup will always be full. By using preprogrammed grasp forces, one must assume the object and hand will be exactly the same between different grasping episodes. Outside of a controlled industrial environment this is an unrealistic assumption: the cup may be of a different size, or the cup may have some water splashed on its rim which could change the friction characteristics. Since the ultimate goal is to lift the cup without crushing despite the presence of uncertainty, online regulation of grasping forces is preferable to using a static predetermined force.

In this paper, we propose a novel force regulation strategy that is particularly suited for precision grasps and objects that are nonrigid, fragile, or with a changing weight. The strategy applies a new slip detection algorithm that is object and hand independent to detect slippage and then compute the required grasping forces that will eliminate this slippage. This strategy can be used for in-hand manipulation as well as simple pick and place operations.

II. Literature Survey

There are generally two modes of slippage in the literature. "Incipient slip" refers to a slip condition where only a portion of the contact location has lost contact. If incipient slip is not corrected, then gross motion between the object and the fingers is likely to occur. This is termed "Gross slip" (or simply "slip"). If slip is not corrected, then the hand loses contact with the object. In this case, either the object drops or "Ejected" or

Manuscript received June 12, 2015; revised October 19, 2015 and February 08, 2016; accepted March 14, 2016. Date of publication April 07, 2016; date of current version October 13, 2016. Recommended by Technical Editor H. Qiao.

The authors are with the School of Engineering, University of Guelph, Guelph N1G 2W1, Canada (e-mail: mstachow@uoguelph.ca; thummel@uoguelph.ca; mmoussa@uoguelph.ca; habdulla@uoguelph.ca).

Color versions of one or more of the figures in this paper are available online at http://ieeexplore.ieee.org.

Digital Object Identifier 10.1109/TMECH.2016.2551557

"reorientation" occurs. "Reorientation" refers to the condition where the object slips but reaches a new, stable configuration in the hand.

A. Overview

Slip detection and correction methods can be broadly broken up into a number of categories. First, the methods can be placed into two types of working principle: vibration-based and object-motion based. Second, slip detectors can use either especially designed sensors or general force/torque contact sensors. Third, the slip detector can detect either gross or incipient slip. Finally, slip correctors can either regulate the grasping force based on the magnitude of slip or by an ad hoc update rule. There can be overlap, however, we have found it useful to use these four dimensions to describe various slip detection and correction methods.

B. Slip Detection Working Principles

Motion between two rough surfaces induces relatively high-frequency signals/vibrations (see, for example, [11]–[15]). These signals are due to the deformation and rubbing of the two materials as contact is made and broken. A number of slip detectors have been developed to observe the frequency content of the contact forces during a slip. Typically these detectors signal slip when the signal switches from predominantly low frequency to predominantly high frequency (see [16]–[18] for early work, and [13] and [19] for a sample of recent discussions on this topic). These signals can be processed by explicitly computing the frequency content of the data (see, for example, [19]), or high-pass filtering of the tactile data (see, for example, [20]).

A number of researchers studying the human sensorimotor system, for example, [21] and [22], have also made this connection. Typically, the sense of touch is broken up into fast adapting and slow adapting type mechanoreceptors. It has been shown that certain types of both receptors are involved in responding to the vibrations induced during slip [21], and that the vibrotactile signals can encode the magnitude of slip as well. Thus, the study of vibrations as a means of detecting slip has a basis in biology.

It is important to note that, by "high frequency," the literature on human and robot grasping considers frequencies that are within the range of 5–100 Hz, compared to the relatively low frequency (0–5 Hz) information that is used for force regulation during stable grasping [20], [21]. Indeed, Romano founded that extremely high slip detection rates can be obtained using information between 5 and 12 Hz [20]. Thus, the challenges of obtaining very high frequency tactile data (above 1 KHz, say) are not present. For the remainder of this paper, when the term "high frequency" is used it is understood to mean that the frequencies are high relative to those needed for force regulation.

Vibration-based methods can suffer from increased sensitivity to robot motion [16]—as the robot vibrates a slip detector may detect spurious slip signals. Methods to reduce this sensitivity to robot motion are not common in the literature. Nonetheless, vibration remains a viable and useful way of detecting slip.

Approaches based on the direct sensing of object motion have also been proposed (for example, [23]–[25]). These approaches have been shown to be able to estimate the magnitude of slip and, in the case of [25], are able to estimate a safety margin of grasping forces before slip takes place. A number of parameters must be set before direct sensing of object motion can be used as a viable slip detection method and periods of experimentation and offline calibration may be needed. Furthermore, it can be difficult to distinguish between real slippage and noise-induced spurious slip signals.

Another issue related to the working principle is how to set the threshold to signal slip. Approaches have been proposed that use offline training/calibration ([19], [26]) or empirically derived thresholds ([20]). offline training or calibration has the disadvantage that a sufficiently rich training dataset must be available, and considerable training time may be needed. Furthermore, it is always possible to have an input that has not been encountered during training, and it is possible that this unfamiliar input will cause incorrect behavior. Using an empirically derived threshold suffers from similar problems. For robots working in unstructured, uncertain environments, a static slip detection threshold may fail in some scenarios, while long training times are undesirable. In these cases, what is required is a slip detection algorithm that adapts its slip detection threshold based on the object's characteristics online and in the context of the current grasp.

Some work has been done on ignoring the detection phase altogether, and directly computing the magnitude of slip as a continuous quantity [23], [24]. This yields a signal that can be used for slip control in interesting ways. Typically this must be done in such a way as to remove spurious signals that may cause a slip controller to activate when slip is not present. In this paper, a similar approach is followed where rather than detecting slip or no-slip, the magnitude of slip is computed as it is occurring.

C. Slip Detection Using Specialized Sensors

Some other approaches to slip detection have focused on designing sensors specifically for slip detection (see, for example, [16], [27]–[31]). Although these methods can be effective for some situations, they typically require periods of calibration. Since the behavior of these sensors may also depend on the object surface properties, different objects will have different responses. Thus, the sensor may need to be recalibrated when encountering new objects. Methods by which general force/torque contact sensors can be used rather than specialized sensors for slip detection are desirable for these reasons.

D. Incipient Slip Detection and Correction

Considerable research has been done on the human response to incipient slip. Humans can sense this incipient slip and modulate grasp forces based on that [32], and a number of robot controllers based on the sensing of incipient slip have been devised.

Many incipient slip detection methods are based on vibration analysis and often require specialized sensors that can directly sense microvibrations at the points of contact (see, for example, [16], [28], and [29]). However, these specialized sensors can suffer from an increased sensitivity to robot motion as with any vibration-based system. Furthermore, many of the specialized sensors are used only for slip, and are unable to sense normal forces. Thus, using them as a slip detection sensor necessitates the use of additional sensors for grasp control. Work has been done to avoid these limitations [33], but the slip detection algorithms presented there require the explicit computation of the frequency content of the tactile data, which requires a very high sampling rate in order to be used for real-time grasp force control. Furthermore, direct observations of the frequency content can be influenced by robot motion regardless. There is a clear need for a slip detection/correction method that is insensitive to robot motion and can be used with a general sensor.

We would also like to note that although it is certainly beneficial to correct for slip before it occurs, sensor limitations may reduce the ability of a robot to use this mode of grasp control. Furthermore, if an incipient slip detector fails to correct the incipient slip, gross motion will still occur. As a result, the proposed method will focus on gross slip and show that with only normal force sensing gross motion can be detected and corrected.

E. Force Regulation and Slip Correction

Slip correction is often treated as a separate problem to slip detection in the literature. A number of slip correction algorithms have been developed that follow the same, very basic principle: when slip is detected, continue to increase the force by a precomputed amount until slip is stopped (see, for example, [20]). These slip correction methods do not consider the magnitude of slip, and thus may cause object reorientation or crushing. Research into methods to consider the magnitude of slip has been proposed but requires the ability to directly sense the motion of the object in the hand, which is not common and requires additional sensors and algorithms for processing (see [23] and [24]).

Additional work in force regulation before slip has been done as well. Some approaches require object models (see, for example, [34] and [35]). Although these approaches tend to perform very well, it is not likely that the robot will have exact object models every time it executes a grasp, especially in unstructured environments. Ito *et al.* [25] proposed a technique to estimate a safety factor between the current grasping force and the minimal grasping force that would induce slip, which could be used as a force feedback variable to prevent slip without an object model. Arimoto proposed a control-theoretic framework for grasping objects without prior information or object models [36], [37], and was able to stabilize the object in the hand before slip occurred. However, Arimoto's method required that the hand have a minimum number of degrees of freedom and could not be used to regulate forces when that minimum was not met. Finally, Stachowsky *et al.* [38] worked toward preslip grasp force regulation, but with a simpler grasp force controller and no ability to handle slip.

III. Contribution and Paper Organization

This paper presents a new strategy for regulating grasping forces during a precision grasp. It employs a new slip detection algorithm that is based on sensing the object in the context of the current grasp, rather than about the object on its own. The slip signals are sourced from multiple tactile sensors in contact with the object. This paper has the following contribution over prior work. There are several important advantages of this strategy over prior work.

1) The slip detection algorithm is calibrated autonomously, online in real time, during a grasp in order to account for object specific parameters.
2) The slip detection is independent of the characteristics of the object being grasped, the gripper design, and the tactile sensor(s) layout. Prior training is not required.
3) The force regulation is closely integrated with the slip detection and is based on the slip magnitude. This makes the force regulation strategy also object independent and operates on the basis of the online real-time calibration.
4) General sensors can be used as long as they are able to sense the normal contact forces, and no explicit computation of the frequency content of the tactile data is necessary. The proposed method is robust to robot motion both theoretically and through experiments.

The remainder of this paper is organized as follows. In Section IV, the strategy is developed from a theoretical standpoint. In Section V, the experimental setup is described, and in Section VI and VII, the experimental results are discussed. Conclusions and future work are presented in Section VIII.

IV. Proposed Approach

A. Context-Specific Force Regulation

The human sensory system generates both feedback data for control as well as internal models for monitoring action. If the information that is sensed differs from the predictions of these models, then reflexive, corrective action is taken [39] using feedback. These models are often rapidly adapted using probing signals.

It has also been shown [39] that the applicability of these internal models is context specific: a model is only effective for a certain range of situations. Practically, this is because the scenarios that a human being will encounter in daily life are vast and varied. A single, unified model will likely not exist for dealing with the environment, and many aspects of the environment are not relevant for a specific task. Thus, the internal models are rapidly calibrated with context limited information. This makes the generation of internal models simpler and faster, obviously at the expense of generality.

For robots, a concept similar to an internal model can be used to calibrate an adaptive mechanism. Since adaptation to a novel scenario might require knowledge of the environment, it would be beneficial to be able to calibrate online as that knowledge becomes available, rather than requiring it to be provided *a priori*.

Finally, note that the goal is not to fully emulate the complexities of the human sensorimotor system since this would require a hand with a sufficiently rich set of sensors and actuators. We are interested in developing a grasp force regulation strategy for hands of any level of complexity, and so have

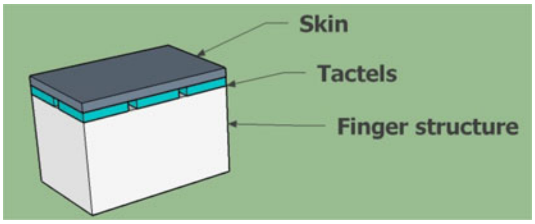

Fig. 1. Schematic setup of fingertip.

chosen to implement key ideas from the study of the human sensorimotor system, and not an emulation of that system in its entirety.

B. Working Principle of Slip Detector

In order to detect slip, the detector uses the force data from at least two tactile elements, or tactels, in contact with the surface. Each tactel may be an individual tactile sensor or possibly a single point of contact in an array force sensor. During no-slip grasping, the tactels should read a constant force corrupted by Gaussian white noise. In particular, note that the noise corrupting one tactel is independent from all of the others. During slip, each tactel will sense the motion of the object's surface. This motion will not be random, and the signal detected at each tactel will no longer be independent. The dependence of the signals from multiple tactels can be observed through the covariance of the signals, and thus, the covariance can be used to detect slip. Sensitivity to noise will be reduced—each tactel will have different noise characteristics but, since the noise is independent for each tactel, the covariance will be small during no-slip grasping. Furthermore, random vibrations due to robot motion will similarly have reduced impact. In what follows, these ideas will be developed further.

Qiao *et al.* [15] studied the characteristics of vibrations induced by slip and determined that the magnitude of vibration depends on the relative velocity of sliding and the vibrations are stochastic non-Gaussian white noise processes.

Point 1 implies that a slip detector that can measure the vibration magnitude during sliding may be able to infer a measure of the magnitude of slip, and to use this measure to compute a control signal that will drive slip to zero. The aforementioned Point 2 implies that, if the robot were to sense this vibration in at least two points on the sliding surfaces, and compute the covariance of these data, the covariance will be nonzero during a slip. This is the main justification for the algorithm developed in this study.

These signals are due to the relative motion of two rough surfaces. In the case of this paper, it is assumed that the fingertip is covered with an elastic skin that can be modeled, for small deflections, as a plate. The skin covers the tactile sensors, which are composed of a number of tactels. The tactile sensors lie between the skin and the finger structure, which is assumed to be rigid (see Fig. 1). The theoretical nature of these signals can be considered by looking at the relationship between the deflections of the plate and the forces that cause those deflections. As the skin and the object surface slide against each other, the roughness of the surfaces will cause deformations in the skin, which in turn gives rise to forces that can be sensed by the tactels.

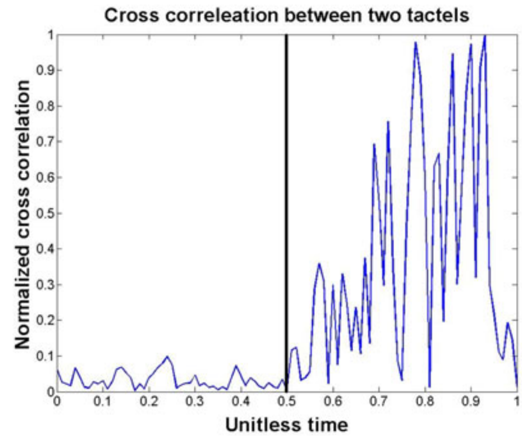

Fig. 2. Cross correlation of two tactels: simulation.

Recall that the relationship between the deformation of a thin, homogeneous plate and the forces that cause that deformation is given by[40]

$$\frac{\partial^4 u(x,y)}{\partial x^4} + 2\frac{\partial^2 u(x,y)}{\partial x^2}\frac{\partial^2 u(x,y)}{\partial y^2} + \frac{\partial^4 u(x,y)}{\partial y^4} = \frac{-f(x,y)}{Q} \quad (1)$$

where $u(x,y)$ is the deformation of the central plane of the plate, $f(x,y)$ is the distribution of transverse load along the plate, and $Q = \frac{2h^3 E}{3(1-\mu^2)}$ with E the Young's modulus, μ the Poisson ratio, and h the distance between one face of the plate and the central plane (i.e., half the plate thickness).

This equation can be used to determine the forces that the tactels will experience as the skin deforms due to rough contact. A MATLAB simulation was performed to test this theory on a generic material ($Q = 1$). Skin deformation was modeled as a stochastic red noise process with fixed (undeformed) edges. The simulation was designed to show that the correlation between two tactels is small when the surfaces are not sliding against each other but is relatively large after sliding occurs. The tactels were assumed to read normal forces only and to be corrupted with Gaussian white noise in order to better determine if sensor noise could cause corruption of results. Fig. 2 shows a plot of the absolute magnitude of the cross correlation between the forces sensed at two tactels. The cross correlation has been normalized. The vertical black line indicates the point at which sliding begins.

To validate this observation, a short experiment was subsequently performed in which an object is grasped and either left in the hand or pulled from the hand (thus, inducing slip). The robot hand was used to grip a juggling ball in a two-finger antipodal pinch grasp, and two sensors were in contact, one on each of the fingertips. The ball was held by the robot 10 cm above the table. To obtain baseline data, the experiment was run with everything held immobile, and data were collected and processed according

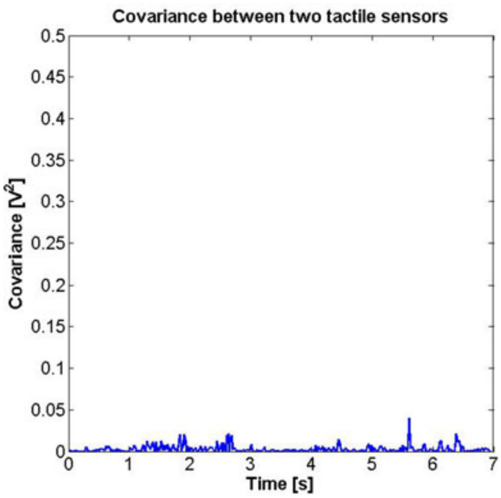

Fig. 3. Covariance between two tactile sensors: no slip.

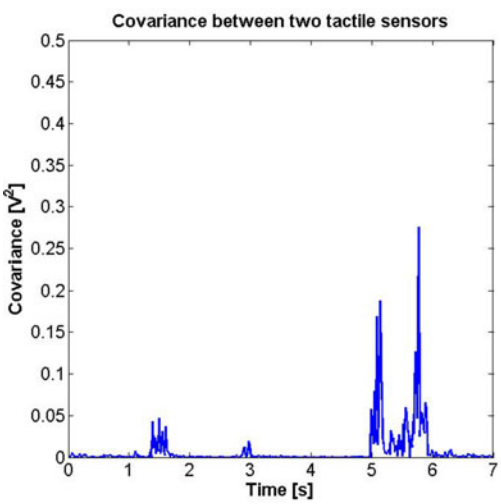

Fig. 4. Covariance between two tactile sensors: slip.

to the algorithm shown below to determine the covariance between the two sensors during a no-slip grasp. We then ran the experiment again, this time pulling the ball from the hand in order to induce slip approximately 5 s into the experiment. Once again the covariance between the two tactile sensors was recorded. Fig. 3 shows the absolute value of the covariance between two tactile sensors during the grasp without slip. Fig. 4 shows the absolute value of the covariance between the same sensors during the grasp with slip. Notice the large spikes in covariance, which agrees with the theoretical observation presented previously.

C. Assumptions

For this study, the following assumptions were made.

1) The object being grasped can be rigid or nonrigid and permanently deformable.
2) No knowledge about the object's mass distribution or friction properties is given.
3) The grasp can be stabilized by an appropriate choice of grasping forces without moving the contact locations.
4) At least two tactile sensing elements are in contact with the portion of the object's surface that is sliding during slip.
5) Normal contact forces can be sensed by tactile sensors on the end effector and are read at a rate sufficient to capture slip.
6) The end effector is capable of modulating grasping forces sufficiently quickly to stop slip as it occurs before ejection or reorientation take place.[1]

TABLE I
TABLE OF SYMBOLS

Symbol	Description
t_k	time step k
$F_i(t_k)$	Normal force reading at contact location i
$d_i^{\max}$	Max value of $\hat{d}$ observed
m	Buffer length
n	Number of contact points
$\vec{D}_i \in \mathbb{R}^{m\times 1}$	Buffer of m previous values of d_i
$\mathcal{H}$	Threshold
β	Threshold-processed output
α	Controller integral gain

D. Description of Variables

Before proceeding, it is useful to summarize the symbols used in this paper. Table I presents the table of symbols. Any further symbols used in the text not defined here will be defined as needed, and generally, represent temporary variables.

We assume that the robot is operating in discrete time. Since, in general, slip may cause inertial loads on the tactile sensors, but these inertial loads will contain most of the low frequency content of the tactile data, this signal will be processed through a high-pass filter to emphasize any high frequency content. To do this, define

$$\hat{d}_i(t_k) = F_i(t_k) - F_i(t_{k-1}). \tag{2}$$

As the numerical derivative of the force sensed at contact location i. Ideally $\hat{d}_i(t_k) = 0$, when the object is in a stable grasp. However, since this a numerical derivative of real sensor data, it is assumed only that $\hat{d}_i$ is Gaussian white noise with zero mean. This being the case, during a stable grasp it follows that the individual variables $\hat{d}_i$ are independent of each other.

We cannot use the $\hat{d}_i$ values directly without proper scaling. This is because the expected no-slip value of $\hat{d}_i$ for each contact location is unknown a priori and may be affected both by the type of sensor that is being used and the object that is being grasped. Thus, before lifting the object the robot will hold the object on the table in a stable grasp with some initial grip force and initiate an online, context-limited calibration phase as discussed

[1]Tremblay suggests that an 80-ms response time is a suitable lower bound to stop slip sufficiently quickly, based on human response times.

in Section IV-A. The calibration is used to generate a set of normalizing constants as follows.

The robot monitors the values of $\hat{d}_i$ for a short time. During this time, the robot will record $d_i^{\max}$, the maximum value for each $\hat{d}_i$ that was encountered during probing. The values of $\hat{d}_i$ are then normalized by this factor online to obtain

$$d_i(t_k) = \frac{\hat{d}_i(t_k)}{d_i^{\max}}. \tag{3}$$

The variables $d_i(t_k)$ will be used to construct a measure of slip for the control program. Since the d_i are simply being scaled by a constant, the assumption that they are independent Gaussian white noise processes during no-slip grasping still holds.

E. Slip Signal Generator

We note that the jth entry in $\vec{D}_i$ is $d_i(t_{k-j})$. Define the matrix $\mathcal{X} \in \mathbb{R}^{m \times n}$ as

$$\mathcal{X}(t_k) := \left[\vec{D}_1; \ \ \vec{D}_2; \ldots \vec{D}_n\right]. \tag{4}$$

Thus, $\mathcal{X}$ is a matrix of the last m values of the n variables $d_i(t_k)$.

Next, define the covariance matrix of the data as

$$\mathbf{\Gamma}(t_k) = \mathcal{X}(t_k)\mathcal{X}(t_k)^T \in \mathbb{R}^{m \times m}. \tag{5}$$

By definition two variables that change together will have a high covariance. If the two variables are independent the covariance between them will be zero [41]. Thus, the assumption that, during a stable grasp, the variables d_i are zero-mean white noise means that $\mathbf{\Gamma}(t_k)$ will be an $m \times m$ diagonal matrix, whose diagonal entries are the variance of the variables d_i, namely σ_i. When the covariance spikes as in Fig. 4, $\mathbf{\Gamma}$ is no longer approximately diagonal.

The slip detection signal will be based off of these nonzero covariances. A formula will be developed that bounds how far from diagonal the matrix $\mathbf{\Gamma}(t_k)$ is, and use that measure to correct for slip.

First, notice that $\mathbf{\Gamma}$ can be rewritten as

$$\mathbf{\Gamma} = \Xi + \mathcal{F} \tag{6}$$

where Ξ is a $m \times m$ diagonal matrix containing the diagonal entries of $\mathbf{\Gamma}$ (i.e., Ξ contains only the variances of the sensor data) and $\mathcal{F}$ is a $m \times m$ matrix such that $\mathcal{F}_{i,i} = 0$ and $\mathcal{F}_{i,j} = \mathbf{\Gamma}_{i,j} \forall i \neq j$.

Recall that the infinity-norm of a matrix, $||\mathcal{F}||_\infty$, is equal to the maximum absolute row sum of the matrix. If $||\mathcal{F}||_\infty \approx 0$ then $\mathcal{F}$ is approximately the zero matrix, and $\mathbf{\Gamma}$ is approximately diagonal. Thus, the algorithm should be designed to coerce $\mathbf{\Gamma}$ to be approximately diagonal.

To do so, define the following quantities:

$$r_i(t_k) = \sum_{j=1}^{m} \left|\mathcal{F}_{i,j}(t_k)\right| \tag{7}$$

and thus

$$||\mathcal{F}||_\infty(t_k) = \max_i r_i(t_k) \tag{8}$$

$||\mathcal{F}||_\infty(t_k)$ is fed back to the slip corrector as the slip signal.

F. Slip Corrector/Grasp Force Regulator

To use the slip signal in a real-time grasping task with slip, an integral controller will be used. The benefit of this update method is that if the original desired force was sufficient to stop slip, then the force does not increase. Due to the integral controller, the steady-state error, $\Xi - \mathbf{\Gamma}$, will be driven to zero [42], and thus, $\mathcal{F} \approx 0$, which is the desired result.

A potential downside to using an integral controller is the problem of integrator wind up. As stated in the assumptions, the sensor derivatives $d_i(t_k)$ are Gaussian white-noise processes when there is no slip. Thus, they are nonzero, which can cause the integrator to continue to increase force even during no slip. To combat this, a threshold, $\mathcal{H}$, is used and a new feedback variable $\beta(t_k)$ defined such that

$$\beta(t_k) = \begin{cases} ||\mathcal{F}||_\infty(t_k), & \text{if } ||\mathcal{F}||_\infty(t_k) > \mathcal{H} \\ 0, & \text{otherwise.} \end{cases}$$

Let $\hat{F}_{\text{des}}$ be the desired grip force in a no-slip situation. Let $F_G(t_k)$ be the updated desired grip force that accounts for any slip conditions. Define $F_G(t_k)$ to be

$$F_G(t_k) = \hat{F}_{\text{des}} + \alpha \sum_{i=0}^{z} \beta(t_k) \tag{9}$$

where α is a gain factor that is derived experimentally. Note that $F_G(t_k)$ is a *desired* grip force. It is assumed that the robot has an internal control loop that is capable of regulating the force once $F_G(t_k)$ is known.

G. Implementation

The final step is to use the initial period of contact as a probing period in order to perform the online calibration. As soon as contact forces stabilize, the vectors $\vec{D}_i$ are filled as force observations become available. At this stage, however, $d_i^{\max}$ is unknown, so no normalization takes place. During a probing period that lasts for a specified amount of time, the contact forces d_i are observed and $d_i^{\max}$ are determined online. Once this probing period is complete, the normalization constants are determined and the online calibration is finished. Thus, the lift may continue. The actual state computation is performed by computing the covariance matrix $\mathbf{\Gamma}$ and the force regulation signal according to the procedure described previously.

V. Experimental Setup

Two sets of experiments were run.

1) *Experiment Set 1:* This set focuses on validating slip detector accuracy and includes two experiments.
   a) Verify slip detection accuracy.
   b) Test algorithm on different robot hand.
2) *Experiment Set 2:* This set focuses on validating the force regulation strategy in real grasping situations and includes four experiments.
   a) Lifting a crushable object.

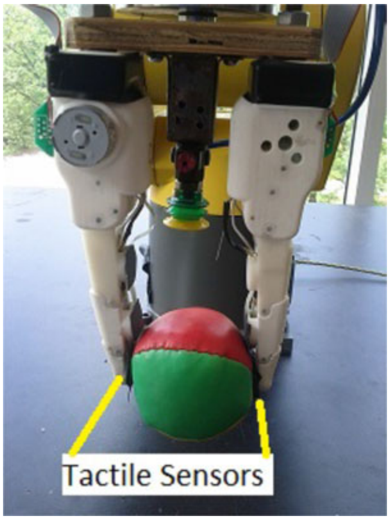

Fig. 5. Hand grasping a ball in two-finger pinch grasp mode (Hand 1).

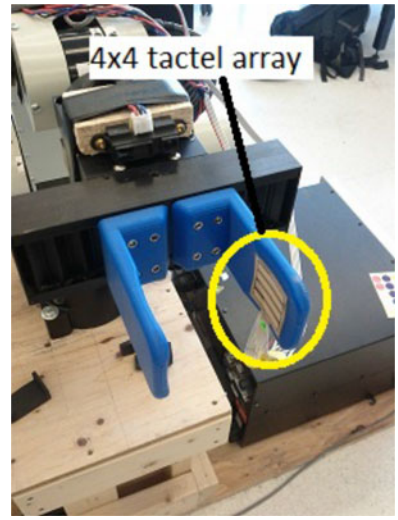

Fig. 6. Second gripper outfitted with tactile array sensors (Hand 2).

b) Lifting the same crushable object with reduced friction.
c) Rejecting robot motion as a source of spurious slip signals.
d) Precision grasping of a fragile object.

In total, six experiments were run using five different materials. The details of each experiment will be given later.

A multifingered, under-actuated hand designed at the University of Guelph's Robotics Institute was used for most experiments. It was controlled by a ChipKit Max32 microcontroller, which was responsible for reading the tactile sensors and encoders and regulating the grasp force once $F_G(t_k)$ was provided. The hand was operated in two-finger pinch grasp mode. The hand was mounted on a Fanuc LRMate 5L robot arm, which is a small human scale arm capable of lifting up to 5 Kg.

Each finger has one force sensitive resistor embedded into each of its three phalanges. They are capable of changing resistance from between 1 MΩ and 100 Ω and read forces between 0.1 and 10 N. They were sampled at a rate of 100 Hz and measure normal forces at the contact locations. Basic calibration was handled from the sensor data sheets. Fig. 5 shows the hand with sensor pads.

A second hand was used in order to validate the extension of the algorithm to multiple tactels and its effectiveness on different robot hands. It is a two-finger pinch gripper with custom 4×4 tactile sensors. These tactile sensors are also able to read contact forces between 0.1 and 10 N, and were also sampled at a rate of 100 Hz. This hand was not able to regulate the force, and thus, was used only for slip detection testing. The second hand is shown in Fig. 6.

A. Tuning Procedure for hand-Specific Parameters and Slip Detection

For all experiments with the hand shown in Fig. 5, the same slip detector setup was used. The parameters are shown in Table II and were arrived at experimentally using the following procedure: A ball was grasped in a two-finger antipodal tip grasp and was held for 3 s before a slip was induced by the experimenter. This experiment was repeated ten times and force data were collected. The parameters $\mathcal{H}$ and m were tuned offline using this data in order to ensure that all ten slips would be detected without any false positives during the static hold phase. The controller gain, α, was then tuned by having the robot grasp the ball with too low a grasping force. The robot lifted until slip occurred, and α was increased until slip was corrected.

TABLE II
PARAMETERS FOR SLIP DETECTOR

Parameter	Value
$\mathcal{H}$	0.05
m	5
n (hand 1)	2
n (hand 2)	16
α	0.1

The parameter n depends on the number of tactels that are available for each contact configuration, and thus, are dependent on hardware design. Hand 1 has two tactels, and thus, $n = 2$ for any experiment that used that hand. When hand 2 (shown in Fig. 6) was used, the parameter n changed to 16, since there are 16 tactels used in the sensor on that hand.

Finally, the following procedure was developed to objectively measure slip. Slip was recorded whenever β was nonzero during a lift. If the object's orientation in the hand was not the same after slip as it was before the grasp, as determined by experimenter inspection, reorientation was recorded. Ejection was recorded if the object was not in contact with the hand at the end of a grasp.

VI. Experiment Set 1: Slip Detection Verification

This experiment set consists of two experiments.

1) Testing slip detection accuracy by inducing slip.
2) Testing the extension of the algorithm to multiple tactels by using a second hand.

TABLE III
CONFUSION MATRIX OF SLIP DETECTOR|

	Class: Slip	Class: No slip
Slip	98%	2%
No Slip	2%	98%

The experiments in this set were run in order to determine the efficacy of the slip detector for use in the force regulation strategy.

For both experiments, the rates of true positive slip signals and true negative slip signals were observed. However, since the slip detector does not output a TRUE/FALSE signal when slip is or is not occurring, define true positives and true negatives as follows.

1) A true positive is recorded when the object that is being grasped is slipping and β is nonzero.
2) A true negative is recorded when the object that is being grasped is *not* slipping and β is zero.

A. Experiment 1a: Testing Slip Detection Accuracy

1) Setup: The hand shown in Fig. 5 was used for this experiment. A rigid ball was placed in the hand. The hand was commanded to hold the ball with a static force of 2 N at each contact point, which was experimentally verified to be a sufficient force to hold the ball against gravity.

2) Procedure: The testing was repeated several times. For each repetition, the following procedure was followed:

The ball was placed in the hand and the online probing input phase was allowed to complete. The ball was held in the hand for three seconds after probing. The ball was then pulled downwards until it was ejected from the hand. The signal β was recorded during the entire repetition. After each repetition the values of β were analyzed and compared to the criteria for true positive and true negative described above. 50 repetitions were run for this experiment.

3) Results: The true positive/true negative results for the experiments with the first gripper were compiled into a confusion matrix, which is shown in Table III.

As can be seen, the accuracy of the detector is very high for both true positive and true negative classifications. Only one repetition out of the 50 did not result in either a true positive or true negative.

Fig. 7 shows the value of $||\mathcal{F}||_\infty$ and a signal that is zero when $||\mathcal{F}||_\infty < \mathcal{H}$ and one when $||\mathcal{F}||_\infty > \mathcal{H}$, in order to show the slip detection proceeding. This figure shows data from a representative experiment taken during the above 50 trials. Notice that, since $||\mathcal{F}||_\infty$ can vary widely during a slip, there are short time periods (usually less than one time step) where the slip signal goes to zero. This behavior is mainly due to the unpredictable nature of the slip vibrations.

B. Experiment 1b: Extension to Multiple Tactels and Different Hands

1) Setup: The hand shown in Fig. 6 was used for this experiment. A rigid ball was placed in the hand. The hand was

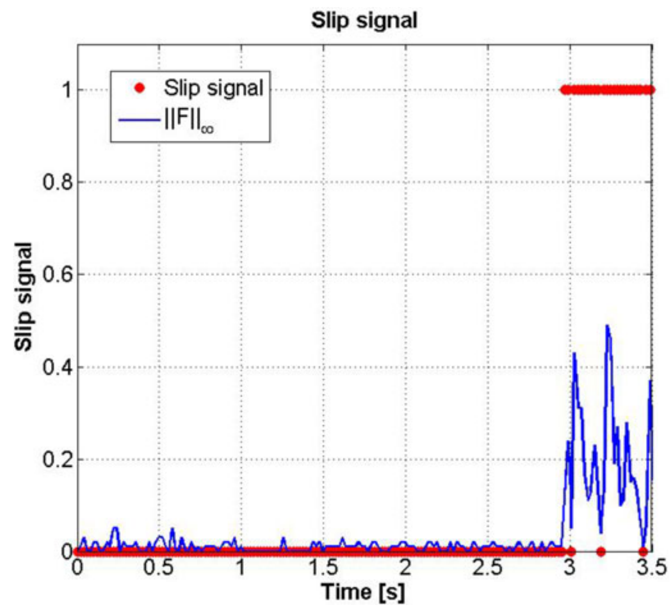

Fig. 7. Slip signal.

commanded to close. This hand does not have the ability to regulate forces, so we were unable to command it to use a static force for holding.

2) Procedure: As before, for each experimental repetition, the following procedure was followed:

The ball was placed in the hand and the online probing input phase was allowed to complete. The ball was held in the hand for three seconds after probing. The ball was then pulled downwards until it was ejected from the hand. For this experiment, the values of β were recorded. After each repetition, the values of β were used to verify the slip detection accuracy of the strategy with different hardware. Fifteen repetitions were run in this experiment.

3) Results: 15/15 slips were successfully detected, resulting in a 100% true positive rate. For testing true negative rate, 1/15 repetitions ended with a false positive reading, resulting in a 93% true negative rate. Thus, using a different hand with considerably different sensor setup did not significantly affect the slip detection accuracy.

VII. EXPERIMENT SET 2: VALIDATION

This experiment set consists of four experiments.

1) Lifting a crushable object with insufficient initial grasping forces: Since the object was crushable it was not acceptable to lift with maximum force. Instead it was assumed that the robot had an initial guess at the grasping force that was too low, and thus the object would slip during the lift. This experiment tested whether slip could be corrected without crushing the object.
2) Lifting a crushable object with uncertain friction properties: Although it is conceivable that a robot operating in a human environment would be required to do repetitive tasks, it is also likely that preprogramming these tasks is not a feasible method of achieving them. In this experiment, the robot's finger friction was altered but the

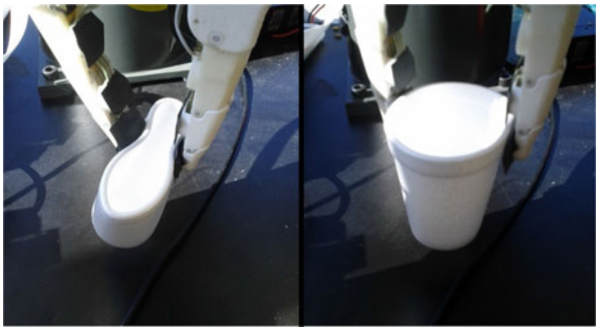

Fig. 8. Cups being gripped with maximum force (left) and with force regulation strategy operating (right).

robot had no knowledge of this. The force regulation strategy's ability to correct for this unknown change was investigated.

3) Lifting an object from the table and rejecting robot motion as a source of spurious slip signals. As stated in the literature review, a potential downside to using high-frequency vibration as a slip signal generation method is that robot motion may induce spurious slip signals. This experiment investigated the sensitivity of the force regulation strategy to robot motion.
4) Lifting a thin, breakable object that can reorient in the hand and be damaged as a result: As stated previously, a key reason to use a force controller in precision grasps that does not grasp with excessive force is to prevent the possibility of reorienting an object in the grasp. This can happen with thin objects lying on a table, which need to be picked up before further manipulation can take place. In these cases, a precision grip is necessary. In this experiment, a common task that a service robot may have to perform was replicated: lifting a fragile food item off of a platter or a tray.

Before proceeding to the first group of experiments, it is important to verify that the crushable object, a Styrofoam cup, could indeed be crushed by the application of too high a grasping force with the hardware that was used in this study. Fig. 8 shows two grasps. On the left, the hand closed with maximum force. On the right, the hand closed with the force regulation strategy operating. Note how the cup is crushed during the lift with maximum force. Thus, this object does require an intelligent choice of grasping forces and cannot simply be lifted with maximum force.

A. Experiment 2a: Lifting a Crushable Object With Insufficient Initial Grasping Forces

1) Setup: A Styrofoam cup was filled with approximately 0.1 Kg of weight and placed on a table. The hand shown in Fig. 5 was commanded to close in a two-finger precision grasp. The initial choice of desired grasping forces was determined through experimentation to be sufficient to lift the cup if it were empty, but not sufficient to lift the cup when full.

2) Procedure: For each experimental repetition, the following procedure was followed.

Fig. 9. Lifting a filled cup without crushing.

Once the hand closed around the cup, the probing input phase was allowed to complete. At that point the robot was commanded to lift the cup vertically by 5 cm. The signal β was recorded during the entire repetition, and was analyzed after the repetition to determine if a slip had occurred. Once the lift ended, the robot was held stationary and whether the cup was crushed or not was observed. Whether the cup was in a stable grasp or not was also observed. Ten repetitions were run for this experiment.

3) Results: In each of the ten experimental repetitions, the cup was successfully lifted without crushing. After observing β it was determined that each repetition began with a slip that was corrected during the lift.

Fig. 9 shows the end of a grasp with the filled cup, after a slip, and Figs. 10 and 11 show the desired and actual cup forces, respectively. Note the spike in desired and actual grasping forces due to the slip event approximately 1.5 s into the grasp.

This experiment has shown that the force regulation strategy presented here is capable of handling slips without crushing a nonrigid object despite an incorrect guess of the initial grasping force.

B. Experiment 2b: Lifting a Crushable Object With Uncertain Friction Properties

1) Setup: As aforementioned, a Styrofoam cup was filled with 0.1 Kg of weight and placed on a table. In order to simulate a reduction in friction characteristics the robot's fingers were coated in water before being commanded to close around the object. The robot was commanded to grip with 3.3 N of force, which was determined to be sufficient to lift the cup when full.

2) Procedure: This experiment proceeded in two rounds.

First, ten repetitions were conducted in which the fingers closed on the cup and the grip force was held static at 3.3 N. The robot was commanded to lift the cup vertically by 5 cm. After the lift whether the grasp was successful or not was recorded.

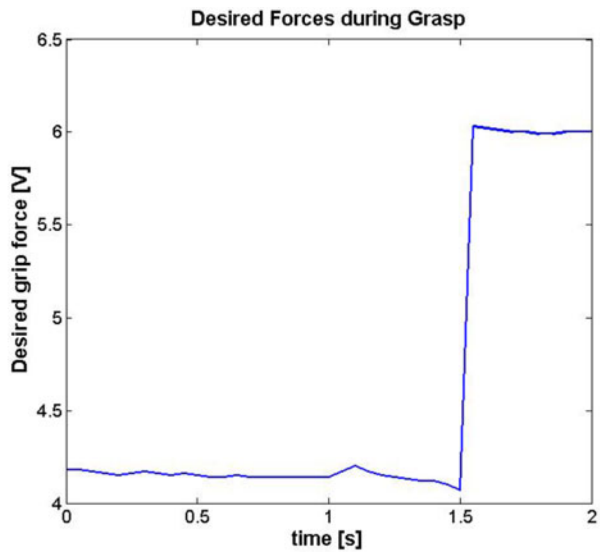

Fig. 10. Desired forces.

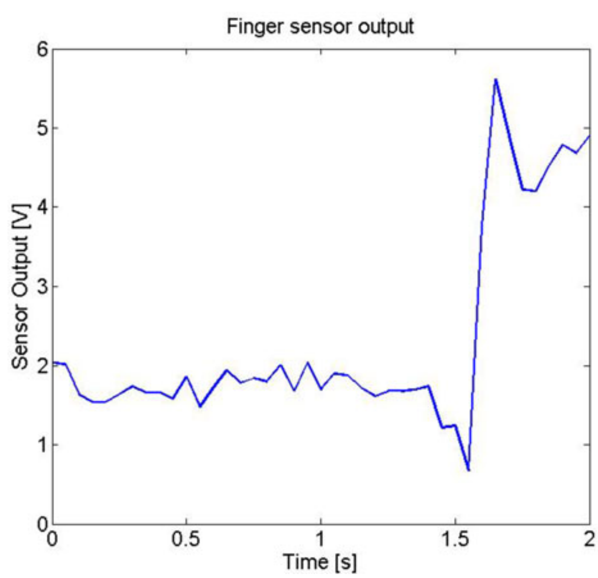

Fig. 11. Actual forces.

TABLE IV
CHANGING FRICTION CHARACTERISTICS

Setup	Successes
Constant Force	2/10
Slip Detector	10/10

Second, the force regulation strategy was turned ON, and the experimental procedure was identical to that in Section VII-A2. Ten repetitions of this experiment were run, and the success of the grasp was recorded.

3) Results: The results are summarized in Table IV.

In cases in which grasp characteristics can change, a pre-programmed solution may not be sufficient. Even though the initial force of 3.3 N was sufficient to lift the object with the original friction characteristics, it was not sufficient when the friction was reduced. The slip detector performed as expected, handling the change in friction properties without any *a priori* knowledge. Thus, unless the robot can predict friction properties, mass distributions, and object durability online in order to better inform a grasp plan, this strategy can be effective even in an environment where the tasks are repetitive.

Fig. 12. Irregularly shaped object (yellow circle indicates desired contact location on one side of object).

TABLE V
STATISTICS FROM INSUFFICIENT FORCE EXPERIMENT

Statistic	Value
Mean desired force increase [%]	40.15
Standard deviation	0.35

Fig. 13. Safe grasping of a damageable food item.

C. Experiment 2c: Testing Sensitivity to Robot Motion

1) Setup: The next experiment tested the ability of the force regulation strategy to reject robot motion and still correct for slip. This experimental proceeded in two rounds with differing setups but identical procedures.

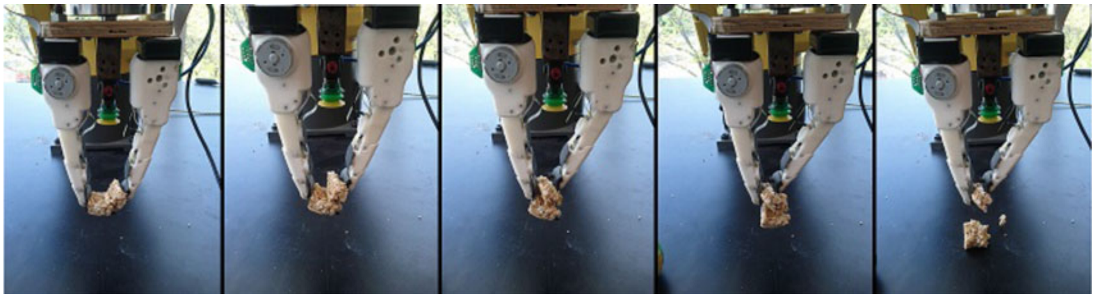

Fig. 14. As the object begins to reorient, it breaks into two pieces and eventually ejects from the hand.

First, the rigid ball was used, and second, an irregularly shaped object, shown in Fig. 12 was used. The robot was placed in position to grasp the object that was on the table, and an initial grasping force was determined offline. The grasping forces used were either 1 N, which is too low to lift either object, or 3 N, which is sufficient to lift the objects.

For each object, the fingers were placed in antipodal tip grasps. In order to achieve this with the irregular object, the object was grasped laterally with the fingers contacting on the two plastic "tabs" that are present on the object (see Fig. 12).

2) Procedure: The object was placed on the table and the hand grasped it in a two-finger pinch grasp. The online probing input phase was then allowed to complete. The robot was commanded to lift the object 5 cm vertically. The signal β was recorded during the entire repetition. After each repetition, the values of β were analyzed and compared to the criteria for true positive and true negative described previously in Section VI. In all, 20 repetitions were run for each object: ten with insufficient initial grasping forces and ten with sufficient forces.

The force regulation strategy's sensitivity to robot motion was evaluated as follows: If the initial grasping force was sufficient to lift the object, then the grasping force should not be commanded to increase more than a predetermined amount during the lift. For this paper, we have empirically chosen to use a maximum allowed increase of 10%. If this was violated in a repetition of the experiment, the force regulation strategy was considered to be sensitive to robot motion for that repetition.

3) Results: When the robot was lifting the ball with insufficient initial guess at the force, all ten repetitions ended in an increase in finger forces and a successful grasp. This result confirms the aforementioned slip detector accuracy experiment. Table V shows the standard deviation, and average percentage increase in desired grasping forces for this experiment. Note that, of course, the increase in desired forces tends to relate to the magnitude of slip.

When the forces were sufficient to grip the object, 90% of repetitions ended without a significant increase in grip force. The increase in grasp force in the one repetition that required that was 12%, which implies that the spurious slip signal was relatively low. All repetitions ended in successful grasps.

When the second object was lifted with a sufficient grasping force, 0/10 repetitions ended in an increase in force, and all ended in a stable grasp. When the object was lifted with insufficient force, slip occurred and was properly detected in all repetitions, further confirming the slip detection accuracy results. However, two failures were observed. In one of the failure repetitions, the fingers slid along the object before the contact forces could stabilize, thus calibration could not take place. In the other failure, the increase in grip force caused the fingers to slide off of the object. Both of these failures imply that assumption 3 in Section IV-C, namely that the grasp can be stabilized against gravity by an increase in grip force, was violated. Thus handling these failures would likely require a higher level regrasp algorithm such as the one presented in [43], and is not necessarily a failure of this strategy.

D. Experiment 2d: Maximum Gripping Force can Cause Object Reorientation and Damage

1) Setup: A granola square was placed in the hand, which was commanded to grip it in a precision grasp.

2) Procedure: This experiment proceeded in two rounds. First, the force regulation strategy was turned ON. After the initial probing phase the robot held the square for 20 s. During this time, the object was observed visually to determine if any deformation or reorientation was occurring. Second, the hand was commanded to grip the square with maximum force and the robot once again held it for 20 s. As before, the object was observed visually to determine if any reorientation occurred.

3) Results: Fig. 13 shows the granola square in a stable, precision grasp without appreciable deformation. In this figure, the grasp force regulation strategy is turned ON, and does not damage the object or cause it to reorient. Fig. 14 shows a sequence of photographs of the object reorienting, and how that reorientation causes eventual breakage of the item. In that sequence, the robot was grasping with maximum force.

Grasping with maximum force is not an appropriate grasp strategy for objects such as the granola square. Because it was thin, lifting it from the table required a precision grasp. As it began to reorient the forces acting on the square were out of balance. Since it was fragile and made of an aggregate material, it had little resistance to these unbalanced forces, and the reorientation of the square caused significant damage. Dealing with scenarios such as this underscores the need for using a reactive grasp force regulation strategy.

E. Comparison With Other Work

In contrast to Romano *et al.* [20], where thresholding and monitoring is required in order to avoid runaway force increases, the proposed strategy uses the slip signal in the feedback loop. Thus, the proposed strategy responds only as much as is necessary—low magnitude slip signals may demand a low magnitude corrective action in order to avoid object damage. Furthermore, the proposed method will respond whenever the slip signal is present, and does not define a regime in which the forces are changing appropriately before correction can take place.

The proposed strategy can also detect slip in real time but without sensitivity to robot motion. This compares favorably with other work [19] and [32].

VIII. Conclusion

The force regulation strategy presented in this paper required no prior object knowledge and can be used with a broad range of objects. The strategy's grounding in a control theoretic framework reduces its reliance on heuristics for recomputing the grasp force, and as long as certain assumptions are met the strategy is successful in eliminating slip without using excessive force.

The use of the slip controller while grasping unknown, possibly fragile objects can go beyond simply correcting an unstable grasp. We can envision a system in which the grasping forces is intentionally set to a very low value and a lift is attempted. When the slip corrector arrests the motion of the object, the normal forces can be analyzed. This will give valuable information about the necessary grasping force for that object and also the friction of the surface at the contact points. These two pieces of information can be used in subsequent grasp attempts. Thus, we believe that this slip corrector could be used in the future to allow for object experimentation for the purposes of grasp planning and analysis.

Beyond grasping of fragile or crushable objects, this strategy can play an important role for in-hand manipulation of small objects during various tasks. Excessive forces applied to the object can result in change of orientation leading to failure of the task while light application of forces can result in slip and task failure as well. Since the proposed method detects slip based on multiple tactile sensors, in the future, we intend to explore ways in which we can extend the method such that manipulation can take place while maintaining stability in the hand. Further, the slip detector can be used to inform finger motion during an in-hand manipulation task.

References

[1] R. Murray, Z. Li, and S. Sastry, *A Mathematical Introduction to Robotic Manipulation*. Boca Raton, FL, USA: CRC Press, 1994.

[2] R. Deimel and O. Brock, "A compliant hand based on a novel pneumatic actuator," in *Proc. IEEE Int. Conf. Robot. Autom.*, 2013, pp. 2047–2053.

[3] P. Sabetian, A. Feizollahi, F. Cheraghpour, S. Moosavian, and K. Toosi, "A compound robotic hand with two underactuated fingers and a continuous finger," in *Proc. 2011 IEEE Int. Symp. Safety, Sec., Rescue Robot.*, 2011, pp. 238–244.

[4] L. Wang, J. DelPreto, S. Bhattacharyya, J. Weisz, and P. Allen, "A highly-underactuated robotic hand with force and joint angle sensors," in *IEEE/RSJ Int. Conf. Intell. Robot. Syst.*, 2011, pp. 1380–1385.

[5] D. Bennet, S. Dalley, D. Truex, and M. Goldfarb, "A multigrasp hand prosthesis for providing precision and conformal grasps," *IEEE/ASME Trans. Mechatronics*, vol. 20, no. 4, pp. 1697–1704, Aug. 2015.

[6] H. Qiao, M. Wang, J. Su, S. Jia, and R. Li, "The concept of "attractive region in environment" and its application in high-precision tasks with low-precision systems," *IEEE/ASME Trans. Mechatronics*, vol. 20, no. 5, pp. 2311–2327, Oct. 2015.

[7] M. Cutkosky, "On grasp choice, grasp models, and the design of hands for manufacturing tasks," *IEEE Trans. Robot. Autom.*, vol. 5, no. 3, pp. 269–279, Jun. 1989.

[8] P. Yu, C. Li, F. Takeda, G. Krewer, G. Rains, and T. Hamrita, "Quantitative evaluation of a rotary blueberry mechanical harvester using a miniature instrumented sphere," *Comput. Electron. Agric.*, vol. 88, pp. 25–31, 2012.

[9] P. Li, S. Lee, and H. Hsu, "Review on fruit harvesting method for potential use of automatic fruit harvesting systems," *Proc. Eng.*, vol. 23, pp. 351–366, 2011.

[10] HDCNews. (2010, Jul./Aug.). [Online] Available: http://www.hdc.org.uk/publication-category/hdc-news

[11] J. Sinou, J. Cayer-Berrioz, and H. Berro, "Friction-induced vibration of a lubricated mechanical system," *Tribol. Int.*, vol. 61, pp. 156–168, 2013.

[12] R. Leine, D. V. Campen, A. De Kraker, and L. Van Den Steen, "Stick-slip vibrations induced by alternate friction models," *Nonlinear Dyn.*, vol. 16, pp. 41–54, 1998.

[13] A. Mazid and A. Ali, "Grasping force estimation detecting slip by tactile sensor adopting machine learning techniques," in *Proc. IEEE Region 10 Conf.*, 2008, pp. 1–6.

[14] A. Le Bot, E. Bou-Choukra, and G. Michon, "Dissipation of vibration in rough contact," *Tibol. Lett.*, vol. 41, pp. 47–53, 2011.

[15] S. Qiao, D. Beloiu, and R. Ibrahim, "Deterministic and stochastic characterization of friction-induced vibration in disc brakes," *Nonlinear Dyn.*, vol. 36, pp. 361–378, 2004.

[16] M. Tremblay and M. Cutkosky, "Estimating friction using incipient slip sensing during a manipulation task," in *Proc. IEEE Int. Conf. Robot. Autom.*, 1993, pp. 429–434.

[17] A. Dutta, G. Muzamdar, V. Shirwalkar, K. Jayarajan, D. Venktesh, and M. Ramakumar, "Development of a dextrous gripper for nuclear applications," in *Proc. IEEE Int. Conf. Robot. Autom.*, 1997, pp. 1536–1540.

[18] E. Holweg, H. Hoeve, W. Jongkind, L. Marconi, C. Melchiorri, and C. Bonivento, "Slip detection by tactile sensors: Algorithms and experimental results," in *Proc. IEEE Int. Conf. Robot. Autom.*, 1996, pp. 3234–3239.

[19] D. Goeger, N. Ecker, and H. Woern, "Tactile sensor and algorithm to detect slip in robot grasping processes," in *Proc. IEEE Int. Conf. Robot. Biomimetics*, 2008, pp. 1480–1485.

[20] J. Romano, K. Hsiao, G. Niemeyer, S. Chitta, and K. Kuchenbecker, "Human-inspired robotic grasp control with tactile sensing," *IEEE Trans. Robot.*, vol. 27, no. 6, pp. 1067–1079, Dec. 2011.

[21] R. Johansson and R. Flanagan, "Coding and use of tactile signals from the fingertips in object manipulation tasks," *Nature Rev. Neurosci.*, vol. 10, pp. 345–359, 2009.

[22] S. Tomlinson, R. Lewis, and M. Carre, "Review of the frictional properties of finger-object contact when gripping," *J. Eng. Tribol.*, vol. 221, pp. 841–850, 2007.

[23] T. Takahashi, T. Tsuboi, T. Kishida, Y. Kawanami, S. Shimizu, M. Iribe, T. Fukushima, and M. Fujito, "Adaptive grasping by multi-fingered hand with tactile sensor based on robust force and position control," in *Proc. IEEE Int. Conf. Robot. Autom.*, 2008, pp. 264–271.

[24] D. Gunji, Y. Mizoguchi, S. Teshigawara, A. Ming, A. Namiki, M. Ishikawaand, and M. Shimojo, "Grasping force control of multi-fingered robot hand based on slip detection using tactile sensor," in *Proc. IEEE Int. Conf. Robot. Autom.*, 2008, pp. 2605–2610.

[25] Y. Ito, Y. Kim, and G. Obinata, "Slippage degree estimation for dexterous handling of vision-based tactile sensor," in *Proc. IEEE Sensors*, 2009, pp. 449–452.

[26] N. Jamali and C. Sammut, "Slip prediction using hidden markov models: Multidimensional sensor data to symbolic temporal pattern learning," in *Proc. IEEE Int. Conf. Robot. Autom.*, 2012, pp. 215–222.

[27] N. Tsujiuchi, T. Koizumi, A. Ito, H. Oshima, and Y. Nojiri, "Slip detection with distributed-type tactile sensor," in *Proc. IEEE/RSJ Int. Conf. Intell. Robots Syst.*, 2004, pp. 331–336.

[28] A. Ikeda, Y. Kurita, J. Ueda, and Y. Matsumoto, "Grip force control for an elastic finger using vision-based incipient slip feedback," in *Proc. IEEE/RSJ Int. Conf. Intell. Robots Syst.*, 2004, pp. 810–815.

[29] H. William, Y. Ibrahim, and B. Richardson, "A tactile sensor for incipient slip detection," *Int. J. Optomechatronics*, vol. 1, pp. 46–62, 2007.

[30] V. A. Ho, D. V. Dao, S. Sugiyama, and S. Hirai, "Development and analysis of a sliding tactile fingertip embedded with a microforce/moment sensor," *IEEE Trans. Robot.*, vol. 27, no. 3, pp. 411–424, Jun. 2011.

[31] D. Damian, T. Newton, R. Pfeifer, and A. Okamura, "Artificial tactile sensing of position and slip speed by exploiting geometrical features," *IEEE Trans. Mechatronics*, vol. 20, no. 1, pp. 263–274, Feb. 2015.

[32] M. Tremblay, W. Packard, and M. Cutkosky, "Utilizing sensed incipient slip signals for grasp force control," presented at the Japan-USA Symp. Flexible Autom., San Francisco, CA, USA, 1992.

[33] M. Schopfer, C. Schurmann, M. Pardowitz, and H. Ritter, "Using a piezo-resistive tactile sensor for detection of incipient slippage," in *Proc. ISR/ROBOTIK*, 2010, pp. 1–7.

[34] Y. Xia, J. Wang, and L.-M. Fok, "Grasping-force optimization for multifingered robotic hands using a recurrent neural network," *IEEE Trans. Robot. Autom.*, vol. 20, no. 3, pp. 549–554, Jun. 2004.

[35] G. Liu, J. Xu, X. Wang, and Z. Li, "On quality functions for grasp synthesis, fixture planning, and coordinated manipulation," *IEEE Trans. Autom. Sci. Eng.*, vol. 1, no. 2, pp. 146–162, Oct. 2004.

[36] S. Arimoto, R. Ozawa, and M. Yoshida, "Two-dimensional stable blind grasping under the gravity effect," in *Proc. IEEE Conf. Robot. Autom.*, 2005, pp. 1196–1202.

[37] S. Arimoto, M. Yoshida, and J.-H. Bae, "Stable blind grasping of a 3-D object under non-holonomic constraints," in *Proc. IEEE Conf. Robot. Autom.*, 2006, pp. 2124–2130.

[38] M. Stachowsky, M. Moussa, and H. Abdullah, "A locally adaptive online grasp control strategy using array sensor force feedback," in *Proc. IEEE/RSJ Int. Conf. Intell. Robots Syst.*, 2012, pp. 4060–4065.

[39] R. Flanagan, K. Merrit, and R. Johansson, "Predictive mechanisms and object representations used in object manipulation," in *Sensorimotor Control of Grasping*. Cambridge, U.K.: Cambridge Univ. Press, 2009, pp. 161–177.

[40] (2014, Sep. 30). Kirchoff plates: Field equations. [Online]. Available: http://www.colorado.edu/engineering/CAS/courses.d/AFEM.d/AFEM.Ch20.d/AF EM.Ch20.pdf

[41] R. Kuehl, *Design of Experiments: Statistical Principles of Research Design and Analysis*. Pacific Grove, CA, USA: Duxbury Press, 2000.

[42] J. Doyle, B. Francis, and A. Tannenbaum, *Feedback Control Theory*. New York, NY, USA: Macmillan Publishing, 1990.

[43] K. Hsiao, S. Chitta, M. Cicoarlie, and E. Jones, "Contact-reactive grasping of objects with partial shape information," in *Proc. IEEE/RSJ Int. Conf. Intell. Robots Syst.*, 2010.

Michael Stachowsky received the B.A.Sc. degree in space engineering, and the M.Sc. degree in earth and space science from York University, Toronto, Canada, in 2008 and 2010, respectively. He is currently working toward the Ph.D. degree with the School of Engineering, University of Guelph, Guelph, Canada.

His research interests include reactive robot grasping, robot control, and control of uncertain systems.

Thomas Hummel received the M.A.Sc. degree in automotive engineering and the Ph.D. degree in industrial automation from the University of Guelph, Guelph, Canada, in 2015.

His research interests include nontraditional automation and food processing automation, as well as the development of novel sensor technologies and processing algorithms to enable automation.

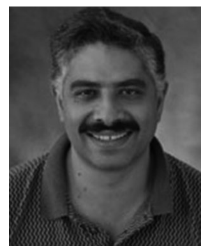

Medhat Moussa received the B.A.Sc. degree in mechanical engineering from the American University in Cairo, Cairo, Egypt; the M.A.Sc. degree in mechanical engineering from the Universite de Moncton, Moncton, Canada; and the Ph.D. degree in systems design engineering from the University of Waterloo, Waterloo, Canada, in 1987, 1991, and 1996, respectively.

He is a Professor with the School of Engineering, University of Guelph, Guelph, Canada. His research interests include robotics grasping, machine vision, machine learning, neural networks, and human–robot interaction.

Dr. Moussa is a member of the Association for Computing Machinery.

Hussein A. Abdullah received the B.Sc. degree in mechanical engineering from the University of Technology, Baghdad, Iraq, in 1981, and the M.Sc. degree in mechanical engineering and the Ph.D. degree in engineering from the University of Glasgow, Glasgow, U.K., in 1988 and 1992, respectively.

He is a Professor with the School of Engineering, University of Guelph, Guelph, Canada. His research interests include rehabilitation robotics, mechatronic systems design, manufacturing systems, and advanced automation and robotics.